frontiers in Plant Science

TYPE Original Research
PUBLISHED 12 November 2026
DOI 10.3389/fpls.2026.1889040

Check for updates

OPEN ACCESS

EDITED BY
Aarti Gupta,
Central University of Kashmir, India

REVIEWED BY
Zareen Sarfraz,
Chinese Academy of Agricultural Sciences, China
Madhvi Sharma,
International Crops Research Institute for the Semi-Arid Tropics (ICRISAT), India

*CORRESPONDENCE
Katharina Anne Scherf
k.scherf.leibniz-lsb@tum.de

RECEIVED 23 May 2026
REVISED 15 July 2026
ACCEPTED 16 October 2026
PUBLISHED 12 November 2026

CITATION
Kaemper C, Lorenz KK, Dietzel T, Siegel K, Knopf O, Muller O and Scherf KA (2026) Proteomic responses to elevated CO_2 in wheat flag leaves are largely cultivar- and year-specific. *Front. Plant Sci.* 17:1889040. doi: 10.3389/fpls.2026.1889040

COPYRIGHT
© 2026 Kaemper, Lorenz, Dietzel, Siegel, Knopf, Muller and Scherf. This is an open-access article distributed under the terms of the Creative Commons Attribution License (CC BY). The use, distribution or reproduction in other forums is permitted, provided the original author(s) and the copyright owner(s) are credited and that the original publication in this journal is cited, in accordance with accepted academic practice. No use, distribution or reproduction is permitted which does not comply with these terms.

Proteomic responses to elevated CO_2 in wheat flag leaves are largely cultivar- and year-specific

Christine Kaemper[1,2], Kim Karolin Lorenz[1,2,3], Tobias Dietzel[1], Kim Siegel[1], Oliver Knopf[4], Onno Muller[4] and Katharina Anne Scherf[1,2,3]*

[1]Department of Bioactive and Functional Food Chemistry, Institute of Applied Biosciences, Karlsruhe Institute of Technology (KIT), Karlsruhe, Germany, [2]Leibniz Institute for Food Systems Biology at the Technical University of Munich, Freising, Germany, [3]TUM School of Life Sciences, Professorship of Food Biopolymer Systems, Technical University of Munich, Freising, Germany, [4]Institute of Bio- and Geosciences: Plant Sciences (IBG-2), Forschungszentrum Jülich GmbH, Jülich, Germany

Increasing atmospheric CO_2 concentrations are expected to alter carbon and nitrogen metabolism in C_3 crops such as wheat (*Triticum aestivum*), affecting not only grain yield and quality but also source tissues involved in assimilate supply. Among these, the flag leaf plays a central role during grain filling. Here, we investigated the effects of elevated CO_2 on protein content and protein composition in flag leaves of ten winter wheat cultivars grown under ambient (≈420 ppm) and elevated (≈600 ppm) CO_2 during the 2021 and 2022 growing seasons. To establish a robust proteomic workflow, four protein extraction methods were compared, identifying filter-aided sample preparation as the most suitable, followed by combined extraction, phenol extraction, and trichloroacetic acid/acetone precipitation. An SDS concentration of ≈0.5% was optimal, whereas higher concentrations markedly reduced protein identifications. Protein content ranged from 1.8 to 3.9% of fresh weight. Three-way ANOVA showed significant cultivar effects and a significant year × CO_2 interaction, but no overall CO_2 main effect, indicating strong environmental modulation of protein responses. Quantitative proteomics confirmed this pattern, with principal component analysis separating samples primarily by year rather than CO_2 treatment or cultivar. Only 22 proteins in 2021 and six proteins in 2022 were significantly altered in more than one cultivar, demonstrating limited common responses. Across all cultivars, 267 and 222 proteins were differentially abundant under elevated CO_2 in 2021 and 2022, respectively, but no pathways were consistently enriched across years. Overall, environmental variability exerted a stronger influence on wheat flag leaf protein metabolism than elevated CO_2 alone, highlighting pronounced genotype × environment interactions.

KEYWORDS
climate change, free-air carbon dioxide enrichment (FACE), Pierce assay, proteomics, Rubisco, *Triticum aestivum*, untargeted LC-MS/MS

1 Introduction

Ambient CO_2 concentrations (aCO_2) in 2025 (≈430 ppm) were higher than at any time during the past two million years (Lan et al., 2026). A further increase in aCO_2 is anticipated, with projections suggesting concentrations may reach up to 1000 ppm by the end of the 21st century, depending on the emission scenario (IPCC, 2023). Given the essential role of wheat in human nutrition, numerous studies have been conducted in recent years to investigate the effects of elevated CO_2 concentrations (eCO_2) on wheat growth and grain composition. Meta-analyses have consistently demonstrated that eCO_2 enhances total plant biomass and grain yield, whereas the protein content of vegetative tissues and grains decreases, thereby reducing the nutritional quality of wheat (Wang et al., 2013; Broberg et al., 2017). A further meta-analysis of C_3 plants demonstrated that phenotypic traits exhibit differential responses to CO_2 (Poorter et al., 2022).

Several explanations have been proposed for the decline in protein content in vegetative tissues under eCO_2. One hypothesis suggests that eCO_2-induced biomass accumulation leads to a dilution of absorbed nitrogen (Taub and Wang, 2008; Wang et al., 2013). Alternatively, eCO_2 may inhibit nitrogen assimilation by limiting the availability of nicotinamide adenine dinucleotide required for nitrate reductase activity (Bloom et al., 2020). At the initial stage of plant carbon metabolism, eCO_2 has been shown to affect photosynthetic processes (Dusenge et al., 2019). Increased CO_2 availability as a substrate for ribulose-1,5-biphosphate carboxylase oxygenase (RuBisCO) stimulates photosynthesis while simultaneously suppressing photorespiration (Drake et al., 1997). However, photosynthetic acclimation refers to the decline in photosynthetic rate following an initial stimulation by elevated eCO_2 (Gámez et al., 2020). This response is associated with sugar accumulation and the down-regulation of photosynthetic proteins, including RuBisCO (Moore et al., 1999).

In wheat, leaves represent the primary site of photosynthesis. During development, a wheat plant typically produces eight to nine leaves, with the final and topmost leaf referred to as the flag leaf. As it provides a substantial proportion of the assimilates required for grain filling, the flag leaf is considered a major determinant of grain development (Song et al., 2025). Accordingly, removal of the flag leaf reduces kernel weight and may lead to grain yield losses of up to 40% (Patterson and Ohm, 1975; Racz et al., 2022). However, eCO_2 has been reported to accelerate flag leaf senescence, potentially limiting its contribution to grain development (Zhu et al., 2009). Moreover, reduced nitrogen concentrations despite increased plant growth have been observed under eCO_2, indicating photosynthetic acclimation (Aranjuelo et al., 2011; Medina et al., 2016). The effects of eCO_2 on protein concentrations in flag leaves are inconsistent, with studies reporting either an increase (Gámez et al., 2020) or a decrease (Aranjuelo et al., 2015).

Taken together, these findings highlight the need for a comprehensive analysis of protein-level responses in wheat flag leaves under eCO_2 conditions. To investigate protein responses, reliable protein extraction methods are required for comprehensive analyses of plant tissues. The most commonly used approaches include trichloroacetic acid (TCA)/acetone precipitation and phenol extraction, as well as a combination of both (Wu et al., 2014). In the TCA/acetone method, proteins are precipitated under acidic conditions, concentrating them while removing phenolics, lipids, and pigments and inhibiting degradative enzymes (Wang et al., 2008). For phenol extraction, the samples are mixed with an alkaline extraction buffer and phenol, resulting in phase separation in which proteins partition into the phenolic phase while water-soluble contaminants remain in the aqueous phase. Proteins are subsequently precipitated with ammonium acetate in methanol. The combined method integrates both procedures and often provides higher protein purity, particularly for plant tissues rich in interfering compounds (Wang et al., 2008; Wu et al., 2014). Filter-aided sample preparation (FASP) uses centrifugal filters with a defined molecular weight cut-off to retain proteins while enabling detergent removal, buffer exchange, and proteolytic digestion on the filter. Peptides generated during digestion are subsequently eluted with high purity (Wiśniewski et al., 2009).

Despite the availability of well-established protein extraction and preparation techniques, proteomic analyses of wheat flag leaves under eCO_2 are still limited in scope. Proteomic analysis by Pandey et al. (2017) identified 50 differentially expressed proteins in leaves grown under aCO_2 and eCO_2, with RuBisCO content being reduced under eCO_2. However, these studies were conducted using only a single cultivar and therefore provide limited insight into potential cultivar-specific responses of flag leaves to eCO_2. Consequently, it remains unclear whether these responses are conserved across modern winter wheat cultivars or whether substantial cultivar-specific differences exist. This study aimed to investigate the protein content and composition of flag leaves collected from ten modern German winter wheat cultivars (*Triticum aestivum*) grown in a Free-Air CO_2 Enrichment (FACE) facility over two years (Knopf et al., 2024). To ensure robust and reproducible proteomic analyses, protein extraction methods were optimized prior to sample characterization.

2 Materials and methods

2.1 Chemicals

All reagents, salts and solvents were obtained from Acros Organics (Geel, Belgium), Alfa Aesar (Ward Hill, MA, USA), Applichem (Darmstadt, Germany), Carl Roth (Karlsruhe, Germany), Honeywell (Charlotte, NC, USA), Thermo Fisher Scientific (Waltham, MA, USA) and VWR Chemicals (Radnor, PA, USA). Trypsin (from bovine pancreas, TPCK-treated, enzyme activity according to manufacturer: ≥10,000 U/mg protein) was obtained from Sigma-Aldrich (St. Louis, MO, USA). Pierce protein assay reagent and Pierce protease inhibitor were obtained from Thermo Fisher Scientific.

2.2 Plant material

The samples used in this study consisted of wheat flag leaves obtained from the BreedFACE project (Knopf et al., 2024). The plants were cultivated in Rheinbach, Germany, at the Campus

Klein-Altendorf experimental field station of the University of Bonn. The project investigated ten different German winter wheat cultivars: Apostel, Asory, Campesino, Foxx, Hyvega, Informer, KWS Emerick, LG Initial, Moschus and RGT Reform.

In the field, the plants were grown under two atmospheric CO_2 conditions: an elevated CO_2 concentration (eCO_2) of approximately 600 ppm and ambient CO_2 concentration (aCO_2) of about 420 ppm as the control (Knopf et al., 2024; Lan et al., 2026). Each wheat cultivar was grown in three plots each under both eCO_2 and aCO_2 conditions. Five to seven flag leaf samples per plot were collected in 2021 and 2022 at stage BBCH60, corresponding to the onset of anthesis and the beginning of grain filling. The leaves collected from each plot were pooled before further processing, with each pooled plot sample representing one biological replicate. After collection, the pooled leaf samples were immediately frozen in liquid nitrogen, stored at −80 °C, and subsequently ground to a fine powder under liquid nitrogen. The resulting leaf powder was stored at −80 °C until further use. Consequently, three independent plot-level biological replicates per cultivar and CO_2 treatment were available for protein and C/N analyses.

2.3 Method development for protein extraction

2.3.1 Trichloroacetic acid/acetone precipitation

The TCA/acetone precipitation was performed based on the protocol of Isaacson et al. (2006), with minor modifications. Approximately 0.15–0.175 g of ground leaf material was weighed in triplicate. For protein precipitation, 2 mL of acetone containing 10% TCA and 0.1% β-mercaptoethanol (β-ME) (v/v) was added, and the samples were vortexed and incubated for 1 h at −20 °C. The samples were centrifuged for 10 min at 2800 relative centrifugal force (rcf) and 4 °C, and the supernatant was discarded. The pellet was washed three times with ice-cold acetone containing 0.1% β-ME (v/v), centrifuged after each wash, and the supernatant removed. The pellet was dried under nitrogen and stored at −80 °C.

2.3.2 Phenol extraction

The phenol extraction was performed based on the protocol of Isaacson et al. (2006), with minor modifications. Approximately 0.15–0.175 g of ground leaf material was weighed in triplicate. The sample was mixed with 2 mL of extraction buffer (0.7 mol/L sucrose, 0.1 mol/L KCl, 0.5 mol/L TRIS-HCl, 50 mmol/L ethylenediaminetetraacetic acid (EDTA), 2% β-ME (v/v), protease inhibitor; pH 8.0) and shaken for 15 min, followed by the addition of 2 mL of phenol and incubation for another 15 min. After centrifugation (10 min, 4 °C, 2800 rcf), the upper phenolic phase was collected and re-extracted with 2 mL of extraction buffer. For protein precipitation, 10 mL of cold precipitation solution (0.1 mol/L ammonium acetate in methanol) was added, and the samples were incubated overnight at −20 °C. The precipitate was recovered by centrifugation, washed twice with precipitation solution and twice with cold acetone, dried under nitrogen, and stored at −80 °C.

2.3.3 Combined extraction

The combined extraction was performed based on the protocol of Wu et al. (2014), with minor modifications. Approximately 0.15–0.175 g of ground leaf material was weighed in triplicate. Two milliliters of 10% TCA/acetone (10% TCA, 0.1% β-ME (v/v) in acetone) were added, and the samples were mixed and centrifuged for 10 min at 4 °C and 2800 rcf (applied to all centrifugation steps). The supernatant was discarded. The pellet was washed twice with the same solution and twice with acetone containing 0.1% β-ME (v/v), dried under nitrogen, and frozen overnight at −20 °C. The pellet was resuspended in 2.5 mL of sodium dodecyl sulfate (SDS) extraction buffer (1% SDS, 0.15 mol/L Tris-HCl, 0.1 mol/L dithiothreitol (DTT), 1 mmol/L EDTA, protease inhibitor; pH 8.5) and incubated for 1.5 h at 22 °C. After centrifugation, the supernatant was collected, mixed with 2 mL of phenol, shaken for 5 min, and centrifuged. The aqueous phase was discarded, and the phenolic phase was washed with wash buffer (10 mmol/L Tris-HCl, 1 mmol/L EDTA, 0.7 mol/L sucrose; pH 8.0), shaken and centrifuged, retaining the phenolic phase. Proteins were precipitated by adding 10 mL of precipitation solution (0.1 mol/L ammonium acetate in methanol), mixing, and incubating overnight at −20 °C. After centrifugation, the pellet was washed with 0.1 mol/L ammonium acetate in methanol and with acetone containing 0.1% β-ME (v/v), dried under nitrogen, and stored at −80 °C.

2.3.4 Resolubilization, reduction, alkylation and digestion

Proteins obtained from TCA/acetone precipitation, phenol extraction, and combined extraction were resolubilized in 1 mL of 50 mmol/L triethylammonium bicarbonate (TEAB) buffer, shaken for 2 min, and centrifuged for 10 min at 22 °C and 2800 rcf. The supernatant was reduced by adding 100 µL of 0.095 mol/L tris(2-carboxyethyl)phosphine (TCEP) in 0.1 mol/L TEAB and incubating at 60 °C for 30 min in a thermoshaker. For alkylation, 100 µL of 0.19 mol/L 2-chloroacetamide (CAA) in 0.1 mol/L TEAB was added, followed by incubation at 37 °C for 45 min in the dark. Samples were dried in a vacuum concentrator at 40 °C and 800 Pa, then resuspended in 1 mL of 0.1 mol/L TEAB containing 0.1 mmol/L sodium deoxycholate. Trypsin solution (50 µL, 0.35 mg/mL; enzyme-to-substrate ratio 1:100) was added, and digestion was performed overnight (≥18 h) at 37 °C in the dark. The reaction was stopped by adding 10 µL of trifluoroacetic acid.

2.3.5 Filter-aided sample preparation

Approximately 0.15–0.175 g of ground leaf material was weighed in triplicate. One milliliter of extraction buffer (2% (w/v) SDS, 1% (w/v) polyvinylpolypyrrolidone (PVPP), 0.1 mol/L TEAB, 10 mmol/L DTT, protease inhibitor) was added. The samples were shaken for 15 min and incubated at 22 °C for 30 min, followed by centrifugation for 10 min at 20,000 rcf. For spin-filter cleanup, 50 µL of the supernatant was applied to the filter, followed by centrifugation for 15 min at 12,500 rcf (applied to all subsequent steps unless stated otherwise). The filter was washed twice with 200

µL of 8 mol/L urea in 0.1 mol/L TEAB, centrifuged after each wash, and the filtrate was discarded. Reduction was performed by adding 50 µL of 0.01 mol/L TCEP in 0.1 mol/L TEAB and 8 mol/L urea, followed by incubation in a thermomixer (500 rpm, 30 min, 60 °C). Alkylation was carried out by adding 50 µL of 0.02 mol/L CAA in 0.1 mol/L TEAB and 8 mol/L urea and renewed incubation (500 rpm, 45 min, 37 °C, darkness). After centrifugation, the filtrate was discarded. The filter was washed with 200 µL of buffer (6 mol/L urea, 3% (w/v) 3-((3-cholamidopropyl) dimethylammonio)-1-propanesulfonate (CHAPS), 0.1 mol/L Tris, 20 mmol/L DTT; pH 7.5), centrifuged, and the step was repeated. For tryptic digestion, 50 µL of trypsin solution (17 µg/mL; enzyme-to-substrate ratio 1:50) were added, and the samples were incubated overnight in a thermomixer (500 rpm, ≥18 h, 37 °C). The peptides were eluted by centrifugation, and digestion was stopped by adding 5 µL of formic acid (FA). The filter was washed twice with 50 µL of 0.1 mol/L TEAB, and the combined eluates were used for solid-phase extraction (SPE).

2.3.6 Solid phase extraction

The peptides were purified by SPE using Discovery DSC-18 SPE 96-well plates with a bed weight of 25 mg per well (Supelco, Sigma-Aldrich). The wells were activated with 1 mL of methanol and equilibrated with 1 mL of 80% (v/v) acetonitrile (ACN) and 0.1% (v/v) FA in water, followed by a wash with 2.5 mL of 2% (v/v) ACN and 0.1% (v/v) FA in water. The samples were loaded onto the wells and allowed to pass through by gravity. The sample tubes were rinsed with 200 µL of 2% (v/v) ACN and 0.1% (v/v) FA in water, and the rinse was applied to the wells and allowed to pass through by gravity. The eluate was reloaded onto the wells and discarded after passing through. The wells were then washed with 2.5 mL of 2% (v/v) ACN and 0.1% (v/v) FA in water. The peptides were eluted using 2 × 50 µL of 40% (v/v) ACN and 0.1% (v/v) FA in water. The eluates were collected, evaporated to dryness (800 Pa, 4–6 h, 40 °C) and stored at -80 °C.

2.3.7 Extraction with different SDS concentrations

Sample preparation was carried out as in section 2.4. During extraction, different buffers containing varying SDS concentrations (0.00%, 0.25%, 0.75%, 1.00%, and 1.50%) were used.

2.3.8 Digestion with different enzyme substrate ratios

Sample preparation was carried out as in section 2.4. Enzymatic hydrolysis was performed using different enzyme-to-substrate ratios (1:50, 1:100, 1:150, and 1:200).

2.4 Final extraction method

Between 70 and 80 mg of frozen leaf powder was weighed in triplicate. Each sample was extracted with 0.5 mL of SDS extraction buffer (0.50% SDS, 1% PVPP, 0.1 mol/L TEAB, 10 mmol/L DTT, protease inhibitor) and vortexed for 5 min, sonicated for 15 min, and incubated at 22 °C for 25 min, followed by centrifugation at 20,000 rcf for 10 min. Fifty microliters of the supernatant were loaded onto a 10 kDa spin filter (Pall Corporation, Port Washington, NY, USA) and centrifuged at 12,500 rcf. The remaining extract was stored at −20 °C. The filter was washed twice with TEAB-urea buffer (8 mol/L urea, 0.1 mol/L TEAB) to remove SDS. Proteins were reduced with 0.01 mol/L TCEP (30 min at 60 °C) and alkylated with 0.02 mol/L CAA (45 min at 37 °C, in the dark). After centrifugation, the samples were washed twice with TEAB-urea buffer and three times with 0.1 mol/L TEAB buffer. To prevent drying during digestion, 400 µL of TEAB buffer was retained in the tube.

For enzymatic digestion, 50 µL of trypsin solution (34 µg/mL in 0.1 mol/L TEAB, enzyme-to-substrate ratio 1:100) was added, and the samples were incubated overnight (≥18 h) at 37 °C in a thermomixer at 250 rpm in the dark. Digestion was stopped by centrifuging the supernatant into a new tube containing 5 µL of FA. Peptides were eluted by two additions of 100 µL 0.1 mol/L TEAB with centrifugation. The samples were evaporated to dryness (800 Pa, 4–6 h, 40 °C) and stored at −80 °C.

2.5 Analysis by nanoLC-MS/MS

For nanoLC-MS/MS analysis, the samples were dissolved in 2% ACN and 0.1% FA in water, adjusted according to sample weight to achieve a constant peptide concentration of 0.2 mg/mL, assuming an average protein content of 2%. Subsequently, 50 µL of this solution was taken and diluted with 750 µL of the same solvent. LC–MS/MS analyses were carried out on a U3000 nanoLC system (Thermo Fisher Scientific) coupled to an Orbitrap Q Exactive Plus mass spectrometer (Thermo Fisher Scientific). Peptide separation was performed on a bioZen XB-C18 nanoLC column (2.6 µm, 250 mm × 0.075 mm; Phenomenex, Torrance, CA, USA) at a flow rate of 0.3 µL/min. The mobile phase consisted of 0.1% FA in water (A) and 0.1% FA in ACN (B). The linear gradient was as follows: 0–5 min, 2% B; 5–6 min, 2–5% B; 6–45 min, 5–20% B; 45–60 min, 20–33% B; 60–62 min, 33–100% B; 62–65 min, 100% B; 65–66 min, 100–2% B; 66–80 min, 2% B. An injection volume of 1.5 µL was applied for samples from 2021, whereas samples from 2022 were analyzed using an injection volume of 15 µL. The column temperature was 40 °C. The loading pump operated in isocratic mode at 100% A with a flow rate of 8.0 µL/min. The spray voltage of the nanoFlex electrospray ionization (ESI) source was 2.8 kV, and the S-lens level was 60. Data-dependent acquisition (DDA) was performed with the following MS1 scan parameters: resolution, 140,000; automated gain control (AGC) target, 3e6; maximum injection time (IT), 50 ms; scan range, *m/z* 300–1300. dd-MS2 scan parameters were: resolution, 17,500; AGC target, 1e5; maximum IT, 100 ms; TopN, 10; isolation window, *m/z* 2.0; fixed first mass, *m/z* 140.0; normalized collision energy, 28; dynamic exclusion, 45 s. The total runtime was 80 min.

2.6 Protein identification

Peptide and protein identification was performed using MSFragger (version 4.4.1) implemented within the FragPipe

(version 23.1) framework (Kong et al., 2017; Teo et al., 2021). The MS/MS raw data were searched against a wheat protein database from UniProtKB (fasta file for organism_id [4565], downloaded on Oct. 16, 2025, 260,812 entries). Oxidation of methionine and N-terminal protein acetylation were specified as variable modifications and carbamidomethylation on cysteines as fixed modification. Trypsin was set as enzyme. MS1-based quantification was enabled using IonQuant, with LFQ and MaxLFQ options activated. In addition, the parameters match between runs and normalize intensity across runs were enabled (Yu et al., 2021). The default settings of the MSFragger Workflow 'Basic-Search' were used for the remaining parameters.

2.7 Protein content

Total protein content was determined using the Pierce assay for the same SDS extracts that were obtained during the FASP procedure (chapter 2.4). Subsequently, 20 µL of the SDS extracts were withdrawn and diluted by adding 60 µL of SDS extraction buffer (0.50% SDS (w/v), 0.1 mol/L TEAB, 10 mmol/L DTT). Then, 150 µL of the Pierce color reagent containing ionic detergent compatibility reagent was added to each sample. In addition, blanks were prepared from the same leaf samples (10 µL of the diluted SDS extract + 150 µL of water) to account for the intrinsic absorbance of the green-colored samples and to subtract this background during the subsequent quantification. The samples were incubated for 5 min at 22 °C before measurement at 660 nm using the Infinite M Nano+ microplate reader (Tecan Group AG, Maennedorf, Switzerland). The calibration curve was generated using 2 mg of bovine serum albumin dissolved in 1 mL of SDS extraction buffer (0.50% SDS (w/v), 0.1 mol/L TEAB, 10 mmol/L DTT). All samples were analyzed in duplicate, and the mean of the two measurements was used.

2.8 C/N content

Total carbon and nitrogen concentrations were determined on finely ground leaf samples using an elemental analyzer (vario EL, Elementar Analysensysteme GmbH, Hanau, Germany) based on dry combustion. The C/N ratio was calculated as the ratio of total carbon to total nitrogen concentrations (mass basis)."

2.9 Statistical analysis

Data analysis and statistics were performed with Excel, version 2016 (Microsoft, Redmond, WA, USA), OriginPro 2023 (OriginLab Corporation, Northampton, MA, USA), Perseus, version 2.1.5.0 (Cox Lab, Munich, Germany) (Tyanova et al., 2016) and R, version 4.5.1 (R Core Team, 2025). Parts of the R scripts used for statistical analysis and data visualization were developed with the assistance of ChatGPT (OpenAI, San Francisco, CA, USA) and subsequently verified, adapted, and executed by the authors.

For protein content data, three-way ANOVA was performed using OriginPro. Differences were considered statistically significant at $p < 0.05$. Label-free quantification (MaxLFQ) data, normalized by MSFragger, were subjected to standardized preprocessing prior to statistical analysis. Proteins annotated as potential contaminants were removed, and values were $\log_2$-transformed. The principal component analysis was performed with the *Principal Component Analysis* App (version 1.63) implemented in OriginPro. Heatmaps were generated using the *Heat Map with Dendrogram* App (version 2.28) implemented in OriginPro. Differential protein abundance analysis was performed in R using the package proDA (Ahlmann-Eltze and Anders, 2019). Differential protein abundance between conditions was assessed using a linear model implemented in proDA. Missing values were handled using the probabilistic dropout model implemented in proDA. To focus on proteins exhibiting substantial changes in abundance, proteins with an adjusted p-value < 0.05 and an absolute $\log_2$ fold change > 1 (corresponding to at least a twofold change) were classified as differentially abundant. Results were visualized using volcano plots generated with the ggplot2 package (Wickham, 2016). The R script used for differential abundance analysis and volcano plot generation has been deposited together with the proteomics dataset in the PRIDE repository (accession PXD078438).

3 Results and discussion

3.1 Method development for protein extraction from flag leaves

Flag leaf samples were processed each in triplicate using TCA/acetone precipitation, phenol extraction, the combined method (collectively referred to as the "classical methods"), and the FASP method employing 10 kDa filter units. A total of 23,952 peptides assigned to 4063 proteins were identified. Among the tested methods, FASP yielded the highest number of identified proteins (2057 proteins, Figure 1A). The combined method resulted in the second-highest number (1783), closely followed by phenol extraction (1727), both corresponding to approximately 85% of the FASP results. In contrast, TCA/acetone precipitation identified 1512 proteins, representing about 74% of the FASP result. At peptide level, the differences between the extraction methods were more pronounced. FASP yielded the highest number of identified peptides (8190), followed by the combined method (6101; 74% of FASP) and phenol extraction (5406; 66%). Consistent with the protein-level data, TCA/acetone precipitation resulted in the lowest number of identified peptides (4410; 54% of FASP).

Duncan et al. (2017) identified 51,043 peptides and 5170 proteins in mature flag leaves using an extraction buffer containing TRIS-HCl, SDS, and β-ME, followed by chloroform/methanol extraction. Their extensive proteome coverage was likely due to peptide fractionation into 12 fractions prior to nanoLC-MS/MS analysis. In contrast, the present study analyzed one single, unfractionated peptide sample, which likely accounts for the lower numbers of identified peptides and proteins. Similarly, Pratap et al. (2025) reported 1,501 proteins in flag leaves also using a chloroform/methanol extraction, which is consistent with the results obtained with the classical extraction methods in this study.

Among the classical extraction methods, TCA/acetone precipitation yielded the fewest peptides, likely due to lower protein purity. Polysaccharides and phenolic compounds co-precipitated

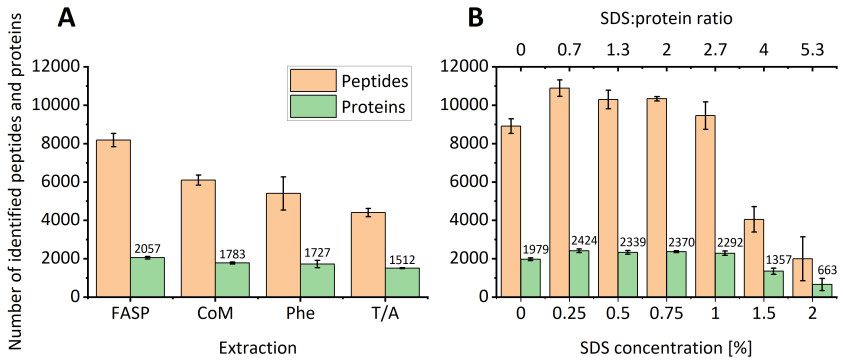


FIGURE 1
Number of identified peptides and proteins in flag leaves of RGT Reform. **(A)** Comparison of four different extraction methods. **(B)** Effect of SDS concentration on peptide and protein group identification. In addition, the SDS-to-protein ratio during extraction is shown, assuming a leaf protein content of 2.5% of fresh weight. CoM, combined method; FASP, filter aided sample preparation; Phe, phenol extraction; SDS, sodium dodecyl sulfate; T/A, trichloroacetic acid/acetone precipitation.

from cell wall material can form complexes with proteins or reduce their solubility. In contrast, phenol extraction inhibits proteolytic enzymes, efficiently solubilizes membrane proteins, and produces cleaner extracts, explaining its higher peptide yield (Wu et al., 2014). Despite the higher variability observed for phenol extraction, the combined method achieved comparable peptide numbers, indicating that increased purification stringency did not impair recovery. Consistent with these findings, Pavoković et al. (2012) reported more protein spots after phenol extraction than after TCA/acetone extraction, attributing this to protein degradation and loss of high-molecular-weight proteins during TCA/acetone treatment. Similarly, Wang et al. (2016) found superior protein recovery with phenol extraction in maize leaves, while the combined method performed slightly worse than TCA/acetone.

Considering peptides (8190) and proteins (2057), the FASP method was best suited for flag leaves. Wang et al. (2018) performed the FASP method with barley leaves and identified over 6000 peptides and approximately 1750 proteins using LC-MS/MS, which agrees with our results. In contrast to conventional extraction methods, where enzymatic digestion is performed in solution, the FASP method involves digestion directly on the filter membrane. Wiśniewski (2016) reported that filter-based digestion is more efficient than in-solution digestion, resulting in a 1.5- to 2-fold higher peptide yield and a 2-fold reduction in peptides with missed cleavage sites (Wiśniewski, 2016). This is also consistent with our findings, as the FASP method yielded by far the highest number of peptides, followed by the combined extraction (74% of FASP), phenol extraction (66%), and TCA/acetone precipitation (54%).

Methodwise, FASP also offers several advantages, including a shorter sample-processing time of approximately 1.5 working days compared to three days for phenol extraction and the combined method. In addition, the procedure is straightforward to perform and does not require the use of toxic chemicals. However, observations during extraction trials revealed that the SDS concentration in the FASP buffer had a marked effect on protein extraction efficiency. Therefore, an additional experiment using different SDS concentrations (0–2.0%) was conducted to investigate the tissue-dependent response of wheat flag leaf proteins to SDS (Figure 1B). Without SDS, 8917 peptides were identified. The highest number (10,892) was obtained at 0.25% SDS. Increasing SDS to 1.00% led to a slight decrease to 10,299 peptides, whereas peptide yields dropped sharply at 1.50% and 2.00% SDS (4056 and 2003, respectively). Similarly, the highest number of proteins was detected at 0.25% SDS (2424). Slightly lower but comparable values were observed at 0.50%, 0.75%, and 1.00% SDS (2339, 2370, and 2292). Fewer proteins were identified without SDS (1979), and markedly reduced numbers were detected at 1.50% and 2.00% SDS (1357 and 663).

Based on the maximum protein content determined for wheat flag leaves (2.5% fresh weight; Pierce assay), SDS-to-protein ratios corresponding to the tested extraction conditions ranged between 0.7:1 and 5.3:1 (Figure 1B). Similar to our observations, Wiśniewski reported reduced peptide recovery at elevated SDS-to-protein ratios in FASP (Wiśniewski, 2019). However, the pronounced decrease in their study occurred only at an 8:1 ratio. In contrast, in our dataset, the decline began already at 4:1. This discrepancy likely reflects matrix-specific effects, as Wiśniewski used mouse brain tissue, while our study examined wheat flag leaves. Furthermore, Wiśniewski recommended an SDS:protein ratio ≥2:1 to exceed the 1.4:1 binding saturation point of SDS and ensure efficient solubilization of membrane proteins. In contrast, our results indicate that this threshold does not benefit wheat leaf tissue: peptide yields were higher below a 2:1 ratio than above it. Nonetheless, extraction without SDS resulted in fewer peptides and protein groups compared with 0.25–1.00% SDS, confirming that SDS is required to enhance protein solubilization and identification. In addition, different enzyme-to-substrate ratios (1:50, 1:100, 1:150, and 1:200) were tested, but they showed almost no effect. Consequently, a ratio of 1:100 was selected for all subsequent analyses.

One limitation of this optimization is that it was performed using only the cultivar RGT Reform, which was selected as an agronomically relevant reference genotype because it is currently one of the most widely grown winter wheat cultivars in Germany. Although the optimized protocol performed successfully across all ten cultivars and generated high-quality proteomic datasets, cultivar-specific differences in leaf composition may influence extraction efficiency. Future studies should therefore assess whether additional optimization is beneficial for other wheat genotypes.

3.2 Analysis of wheat flag leaves from the BreedFACE experiment

The analyses of the protein content (Section 2.7) and proteome (Sections 2.4–2.6) were performed on flag leaves from ten wheat cultivars of the BreedFACE project collected in the 2021 (Knopf et al., 2024) and 2022 growing seasons.

3.2.1 Impact of eCO_2 on flag leaf protein content

The protein content ranged from 1.8–3.9% in 2021 and 2.0–3.8% in 2022 and differed among both years and cultivars (Figure 2A). In 2021, eCO_2 increased protein content in four cultivars (Apostel, Asory, Hyvega, and KWS Emerick), had no effect in five cultivars (Foxx, Informer, LG Initial, Moschus, and RGT Reform), and reduced protein content only in Campesino. In contrast, in 2022 the response to eCO_2 was either neutral or negative across all wheat cultivars. Apostel and Hyvega appeared particularly sensitive to eCO_2 in terms of total protein content. In summary, the results showed negative CO_2 effects in 2022 but diminished or reversed effects in 2021. Three-way ANOVA confirmed significant effects of cultivar and a significant year × CO_2 interaction, but no overall main effect of CO_2 (Supplementary Table S1). Cultivar differences were highly significant, and a significant year × cultivar interaction indicated variable year-to-year responses among cultivars. In contrast, neither the CO_2 × cultivar interaction nor the three-way interaction was significant, suggesting that the CO_2 response was not consistently cultivar-specific but rather depended strongly on year-specific environmental conditions.

Vicente et al. (2019) reported crude protein concentrations of 2.3% of fresh weight (FW) under eCO_2 and 3.4% of FW under aCO_2, which is in line with our study. In contrast, Aranjuelo et al. (2015) found markedly lower protein contents at the onset of grain filling, reporting 0.5% FW under eCO_2 and 0.6% FW under aCO_2. Notably, both studies investigated flag leaves of durum wheat. While both reported a decline in protein concentration under eCO_2, our results showed a partially contrasting trend that varied between cultivars and years. This suggests that environmental conditions, in interaction with genotype, may modulate the CO_2 response. Similarly, other studies have demonstrated that the responses to water stress and eCO_2 are genotype-dependent (Medina et al., 2016). Interestingly, Aranjuelo et al. also reported an increase in protein concentration under eCO_2 in a separate study, further highlighting the complexity of genotype- and environment-specific responses (Aranjuelo et al., 2011).

The plants were grown at the same site, but the weather conditions differed markedly between the two years. Mean January–May temperatures were 6.3 °C in 2021 and 8.4 °C in 2022, with corresponding precipitation totals of 226.7 mm and 191.8 mm, respectively (meteorological station Weilerswist-Lommersum, German Weather Service, 2023). Thus, 2022 was not only warmer but also drier than 2021. These interannual

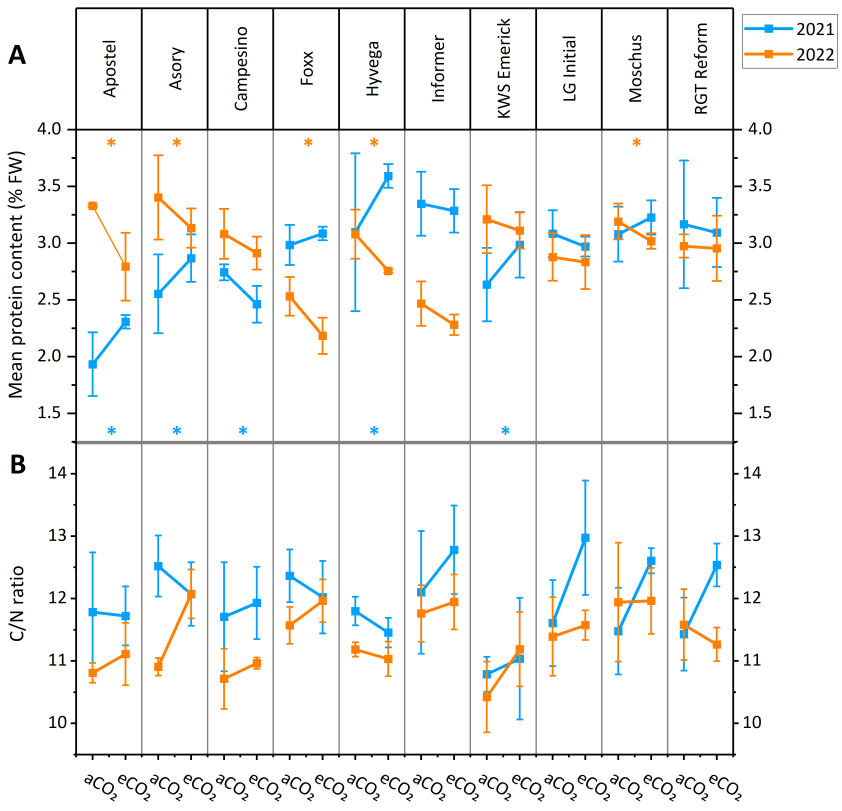


FIGURE 2
Interaction plot of protein content **(A)** and C/N ratio **(B)** illustrating the effects of CO_2 treatment across years and cultivars. *Blue and orange asterisks denote significant differences between ambient and elevated CO_2 treatments within the 2021 and 2022 growing years, respectively ($p < 0.05$). aCO_2, ambient CO_2 concentration; eCO_2, elevated CO_2 concentration; FW, fresh weight.

differences in temperature and precipitation likely contributed to the pronounced environmental effects observed in our study. Our results indicate that the relationship between plants and eCO_2 is more complex, particularly under additional stress factors such as heat (Ekele et al., 2025). In contrast, an earlier study reported that eCO_2 did not affect protein concentrations in plants. The authors attributed this finding to optimal nitrogen availability in the soil, suggesting that sufficient nitrogen supply can compensate for potential CO_2-induced reductions in protein concentration (Idso and Idso, 2001). Another possible explanation for the contrasting results is the sampling time. Our samples were collected at the onset of grain filling, a developmental stage at which nitrogen remobilization from leaves to the developing grains has already begun. At this point, the initial phase of leaf protein degradation may have influenced the measured protein concentrations. This is particularly relevant because it has been reported that leaf senescence can be accelerated under eCO_2, potentially leading to an earlier decline in leaf nitrogen and protein content (Zhu et al., 2009).

Mechanistically, eCO_2 enhances carbon assimilation, which can alter the source–sink balance and the C/N ratio within the plant (Taub and Wang, 2008). An increased carbon supply without a proportional increase in nitrogen uptake may induce adjustments in nitrogen metabolism, including down-regulation of photosynthetic proteins such as RuBisCO, which represent a major nitrogen pool in leaves. Consequently, changes in protein concentration under eCO_2 may reflect not only altered nitrogen availability but also shifts in nitrogen partitioning and remobilization. Consistent with this assumption, the C/N ratio showed a reproducible numerical increase under eCO_2 in both growing seasons. When all cultivars were pooled within each year, mean C/N increased from 11.76 under aCO_2 to 12.08 under eCO_2 in 2021 (+2.8%), and from 11.23 to 11.51 in 2022 (+2.5%). However, these shifts remained marginally above the threshold of statistical significance in year-wise t-tests (2021: $p = 0.090$; 2022: $p = 0.072$). In contrast, protein content did not show a consistent response to eCO_2: when averaged across cultivars within each year, mean protein content increased slightly from 2.9% to 3.0% in 2021, but decreased from 3.0% to 2.8% in 2022. At the cultivar level, the direction and magnitude of the C/N response varied, and after correction for multiple testing, no individual cultivar showed a robust CO_2 effect (Figure 2B). Thus, the C/N data support a general trend toward relatively greater carbon accumulation than nitrogen accumulation under eCO_2, but also indicate that this response was modest compared with the variation attributable to year and cultivar.

3.2.2 Impact of eCO_2 on flag leaf protein composition

To disentangle the effects of eCO_2 from environmental variability, the impact of CO_2 enrichment on flag leaf protein composition was assessed. Principal component analysis (Figure 3) of the proteomics data revealed a clear separation of the samples by growing year, indicating that year-to-year variability exerted a stronger influence on the proteome than eCO_2, as was already observed for total protein content (see Discussion for a consideration of contributing environmental and technical factors). No distinct clustering associated with CO_2 treatment was detected within year-specific groups. Likewise, no clear separation between cultivars was observed.

To further identify individual proteins contributing to the observed proteomic differences, differential abundance analysis was performed and visualized using volcano plots. Accordingly, each cultivar was compared between control and eCO_2 conditions for each growing year (Supplementary Figures S1–S11). Across all wheat cultivars, a total of 267 proteins were significantly differentially abundant in 2021 (Supplementary Table S2). The number of affected proteins varied markedly among cultivars, ranging from one differentially abundant protein in LG Initial to 150 in KWS Emerick. Notably, only 22 proteins were significantly differentially abundant in more than one wheat cultivar, and only a single protein showed consistent differential abundance across four cultivars under the experimental conditions. In 2022, a total of 222 proteins were identified as significantly differentially abundant across all wheat cultivars, with the number of responsive proteins ranging from 109 in Asory to none in Moschus (Supplementary Table S3). Notably, only six proteins were significantly differentially abundant in two different wheat cultivars, indicating a largely cultivar-specific proteomic response. When comparing differentially abundant proteins between the two growing seasons within the same wheat cultivar, virtually no overlap was observed. Apart from one single protein (Protein ID: A0A1D5UPW1 in RGT Reform), no proteins were shared between years. Notably, this protein was downregulated under eCO_2 conditions in 2021 but upregulated in 2022. These findings further indicate that growing year had a stronger influence on the observed proteome than the eCO_2 treatment. It should be noted that, besides genuine inter-annual environmental variability, a technical factor (different LC-MS injection volumes between seasons: 1.5 µL in 2021 vs. 15 µL in 2022) may also have contributed to the pronounced year-based separation observed in the PCA (Figure 3). The PCA was based on normalized MaxLFQ intensities and included only proteins detected in both growing seasons. Nevertheless, we do not assume that normalization and restricting the analysis to shared proteins completely eliminated technical differences between years. As injection volume was constant within each year across both CO_2 treatments, it cannot confound the ambient-vs.-eCO_2 comparisons underlying our differential abundance analysis. Its influence is therefore limited to the between-year comparison and does not affect the within-year treatment comparisons on which our biological conclusions are based.

In 2021, eCO_2 induced cultivar-specific proteomic differences with both up- and down-regulation across functional categories (Supplementary Table S4). The responses prominently involved photosynthesis/chloroplast proteins, carbon and nitrogen metabolism, protein turnover/proteostasis, redox and defense pathways, and regulatory proteins (RNA-/chromatin-associated). While one cultivar (Apostel) showed predominantly up-regulation of metabolic and proteostasis-related proteins, others (e.g., Hyvega, KWS Emerick, Moschus) exhibited broad down-regulation across multiple pathways, consistent with CO_2-dependent acclimation and context-dependent metabolic adjustment. In contrast, Asory, Campesino, Foxx, and LG Initial were largely unaffected, with only two to four proteins showing significant changes under

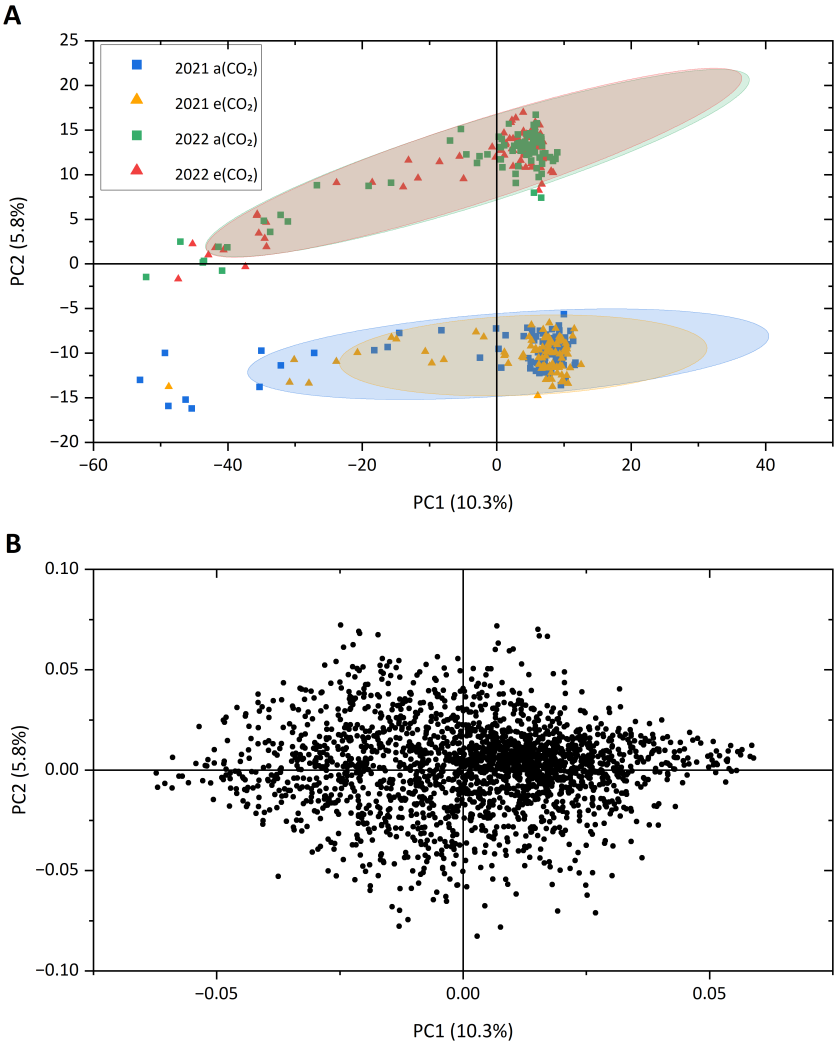


FIGURE 3
Principal component analysis (PCA) of the proteomic dataset reveals a clear separation of samples according to the two growing years. The score plot **(A)** shows distinct clustering along PC1 (10.3% explained variance) and PC2 (5.8%), indicating global proteomic differences between the years. No distinct effect of eCO_2 is apparent within the year-specific clusters. The corresponding loading plot **(B)** indicates that the observed separation is driven by the combined contributions of multiple proteins rather than by a single dominant feature a(CO_2), ambient CO_2 concentration; e(CO_2), elevated CO_2 concentration.

eCO_2 conditions. In 2022, eCO_2 was associated with changes in proteins related to photosynthesis/chloroplast function and energy metabolism, as well as central carbon metabolism, protein turnover, and redox/defense pathways (Supplementary Table S4). In addition, several regulatory proteins (e.g., RNA-binding and chromatin-associated factors) responded to eCO_2, suggesting adjustments at both metabolic and post-transcriptional levels. Response patterns varied among cultivars. Most cultivars exhibited broad downregulation (Asory, Hyvega, Informer, and LG Initial), while Apostel, Campesino, and RGT Reform displayed only a limited number of protein changes. Foxx and KWS Emerick showed almost no significant changes, and Moschus showed none.

Proteomics analyses of wheat leaves collected at anthesis from a CO_2-enriched greenhouse (700 µmol mol^{-1} CO_2) showed that RuBisCO content did not increase. In contrast, the abundance of RuBisCO activase was slightly elevated (Aranjuelo et al., 2015). In our study, however, increased RuBisCO activase abundance was observed exclusively in Campesino in 2021, suggesting a cultivar- and year-specific response rather than a consistent upregulation under eCO_2 conditions. Furthermore, under FACE conditions, leaves were reported to contain less RuBisCO but higher levels of mitochondrial NAD-dependent malate dehydrogenase, indicating alterations in respiratory metabolism and potentially increased respiratory CO_2 loss (Pandey et al., 2017). In our study, this enzyme was not significantly affected in any of the cultivars. Instead, we observed cultivar- and year-specific regulation of a small set of proteins associated with mitochondrial oxidative phosphorylation. Components of the mitochondrial electron transport chain were predominantly downregulated, with NADH dehydrogenase (Complex I) affected in Asory (2022) and a Complex III-associated subunit in Informer (2022). Likewise, mitochondrial ATP synthase subunits (Complex V) showed reduced abundance in Apostel (2022) and LG Initial (2022). Additional cultivar-specific responses included downregulation of a Rieske iron–sulfur protein (Complex III) in Apostel, upregulation of a ubiquinol–cytochrome c reductase 6.7 kDa subunit (Complex III) in Apostel, pronounced

downregulation of Complex III subunit 9 in KWS Emerick, and downregulation of an ATP synthase-related "H(+)-transporting two-sector ATPase" subunit in Moschus. Overall, these patterns point to cultivar- and component-specific adjustments of mitochondrial energy metabolism rather than a consistent stimulation of respiratory flux under eCO_2. Furthermore, KEGG pathway analysis showed that most proteins were associated with metabolic pathways under both ambient and eCO_2 conditions in both years. In contrast, enrichment analysis did not reveal any pathways significantly enriched in both years, most likely because the number of differentially abundant proteins was small and their composition was inconsistent between years.

The decline in photosynthetic efficiency (Fq'/Fm') observed under eCO_2 during later growth stages (Knopf et al., 2024) may reflect a down-regulation of photosynthetic proteins such as RuBisCO, which constitute a major fraction of leaf nitrogen and protein content. A reduction in RuBisCO content under eCO_2 has also been reported in other studies (Aranjuelo et al., 2011; Pandey et al., 2017). Within our dataset, the RuBisCO large chain protein was downregulated in Hyvega, KWS Emerick, and RGT Reform, whereas it was upregulated in Moschus in 2021. In contrast, no significant regulation of the RuBisCO large chain was detected in 2022. However, this regulation alone cannot account for the CO_2-induced changes in leaf protein concentrations observed in our dataset, since Hyvega and KWS Emerick showed increased total leaf protein content under eCO_2 in 2021 (see Figure 2, Chapter 3.2.1), despite the downregulation of RuBisCO large chain. Furthermore, although multiple RuBisCO large and small subunit isoforms as well as RuBisCO activase isoforms were identified, their abundance patterns were inconsistent across cultivars and growing seasons. The corresponding heatmaps did not reveal coordinated regulation of RuBisCO-associated proteins under elevated CO_2 (Supplementary Figures S12, S13; Supplementary Table S5). Together, these findings suggest that the observed variation in RuBisCO abundance reflects heterogeneous genotype- and environment-dependent responses rather than a uniform photosynthetic acclimation. The relatively small differences in RuBisCO-associated proteins between 2021 and 2022 in RGT Reform suggest that temporal (year) effects outweighed the impact of CO_2 conditions (Supplementary Figure S14). This is consistent with the study by Aranjuelo et al. (2015), who also did not observe a significant change in RuBisCO content.

4 Conclusion

The results of the BreedFACE experiment demonstrate that the effects of eCO_2 on wheat flag leaf protein content and proteome composition are highly variable and strongly influenced by environmental conditions. The establishment of an optimized proteomic workflow provided a reliable analytical basis for detecting these responses across cultivars and years. Despite this robust methodological approach, no uniform effect of eCO_2 on protein content or proteome composition was observed. While several cultivars showed increased protein content under eCO_2 in 2021, responses in 2022 were mostly neutral or negative, and no overall CO_2 effect was detected. Proteomic analyses revealed strong year-dependent differences but no consistent separation according to CO_2 treatment. Differential abundance analysis further demonstrated that most eCO_2-responsive proteins were unique to individual cultivars and growing seasons, with only very limited overlap of significantly regulated proteins across cultivars or between years. This lack of reproducible protein responses suggests that elevated CO_2 did not induce a conserved proteomic response under the conditions investigated. Although numerous proteins responded to eCO_2 within individual cultivars, these responses were largely cultivar- and year-specific, with no consistent regulation of key photosynthetic proteins such as RuBisCO. Within the two growing seasons investigated, these findings indicate that year-specific environmental conditions exerted a stronger influence on wheat flag leaf protein composition than eCO_2 alone. However, because this study was limited to two growing seasons, these observations should not be generalized without validation in longer-term experiments encompassing a broader range of environmental conditions. Taken together, these findings indicate that environmental variability exerts a stronger influence on wheat flag leaf protein composition than eCO_2 alone. The pronounced year-to-year differences observed in both protein content and proteomic profiles highlight the complexity of predicting plant physiological responses under future climate scenarios, where eCO_2 will interact with additional environmental stressors such as heat and drought. These results emphasize the importance of considering genotype-environment interactions when evaluating wheat responses to rising atmospheric CO_2 and identifying cultivars with improved resilience to future climatic conditions.

Data availability statement

The mass spectrometry proteomics data have been deposited to the ProteomeXchange Consortium via the PRIDE (Deutsch et al., 2023; Perez-Riverol et al., 2025) partner repository with the dataset identifier PXD078438 (https://www.ebi.ac.uk/pride/archive/projects/PXD078438).

Author contributions

CK: Conceptualization, Data curation, Formal analysis, Investigation, Methodology, Supervision, Visualization, Writing – original draft. KL: Data curation, Formal analysis, Investigation, Methodology, Visualization, Writing – original draft. TD: Data curation, Formal analysis, Investigation, Methodology, Visualization, Writing – original draft. KS: Data curation, Formal analysis, Investigation, Visualization, Writing – original draft. OK: Data curation, Formal analysis, Project administration, Resources, Writing – review & editing. OM: Funding acquisition, Project administration, Resources, Writing – review & editing. KAS: Conceptualization, Funding acquisition, Project administration, Resources, Supervision, Writing – review & editing.

Funding

The author(s) declared that financial support was received for this work and/or its publication. The project was supported by funds of the Federal Ministry of Food and Agriculture (BMEL) based on a decision of the Parliament of the Federal Republic of Germany via the Federal Office for Agriculture and Food (BLE) under the innovation support program. Project number 2818404B18 (BigBaking). Measurements at the Q Exactive Plus Orbitrap mass spectrometer were funded by the Deutsche Forschungsgemeinschaft (DFG, German Research Foundation), project number 445432254. Co-funded by the European Union (ERC, GLUTENOMICS, 101040437).

Acknowledgments

The authors thank Jennifer Pelikan from the Jülich Research Centre, Germany, for performing the CN analyses.

Conflict of interest

Authors OK and OM were employed by company Forschungszentrum Jülich GmbH.

The remaining author(s) declared that this work was conducted in the absence of any commercial or financial relationships that could be construed as a potential conflict of interest.

Generative AI statement

The author(s) declared that generative AI was used in the creation of this manuscript. During the preparation of this work, the first author employed ChatGPT (OpenAI) to assist with language refinement and grammatical corrections, as well as with the generation and optimization of R scripts for statistical analyses and data visualization. All scripts were reviewed, tested, and executed by the authors, who verified all analytical outputs. After using this tool/service, the authors reviewed and edited the manuscript as needed and take full responsibility for the content of the published article.

Any alternative text (alt text) provided alongside figures in this article has been generated by Frontiers with the support of artificial intelligence and reasonable efforts have been made to ensure accuracy, including review by the authors wherever possible. If you identify any issues, please contact us.

Publisher's note

All claims expressed in this article are solely those of the authors and do not necessarily represent those of their affiliated organizations, or those of the publisher, the editors and the reviewers. Any product that may be evaluated in this article, or claim that may be made by its manufacturer, is not guaranteed or endorsed by the publisher.

Author disclaimer

Views and opinions expressed are however those of the author (s) only and do not necessarily reflect those of the European Union or the European Research Council Executive Agency. Neither the European Union nor the granting authority can be held responsible for them.

Supplementary material

The Supplementary Material for this article can be found online at: https://www.frontiersin.org/articles/10.3389/fpls.2026.1889040/full#supplementary-material

References

Ahlmann-Eltze, C., and Anders, S. (2019).proDA: probabilistic dropout analysis for identifying differentially abundant proteins in label-free mass spectrometry. Available online at: https://www.biorxiv.org/content/10.1101/661496v2 (Accessed April 30, 2026). Preprint.

Aranjuelo, I., Cabrera-Bosquet, L., Morcuende, R., Avice, J. C., Nogués, S., Araus, J. L., et al. (2011). Does ear C sink strength contribute to overcoming photosynthetic acclimation of wheat plants exposed to elevated CO2? *J. Exp. Bot.* 62, 3957–3969. doi: 10.1093/jxb/err095

Aranjuelo, I., Erice, G., Sanz-Sáez, A., Abadie, C., Gilard, F., Gil-Quintana, E., et al. (2015). Differential CO_2 effect on primary carbon metabolism of flag leaves in durum wheat (*Triticum durum* Desf.). *Plant Cell Environ.* 38, 2780–2794. doi: 10.1111/pce.12587

Bloom, A. J., Kasemsap, P., and Rubio-Asensio, J. S. (2020). Rising atmospheric CO_2 concentration inhibits nitrate assimilation in shoots but enhances it in roots of C_3 plants. *Physiol. Plant* 168, 963–972. doi: 10.1111/ppl.13040

Broberg, M., Högy, P., and Pleijel, H. (2017). CO_2-induced changes in wheat grain composition: meta-analysis and response functions. *Agron.* 7, 32. doi: 10.3390/agronomy7020032

Deutsch, E. W., Bandeira, N., Perez-Riverol, Y., Sharma, V., Carver, J. J., Mendoza, L., et al. (2023). The proteomeXchange consortium at 10 years: 2023 update. *Nucl. Acids Res.* 51, D1539–D1548. doi: 10.1093/nar/gkac1040

Drake, B. G., Gonzàlez-Meler, M. A., and Long, S. P. (1997). More efficient plants: a consequence of rising atmospheric CO_2? *Annu. Rev. Plant Physiol. Plant Mol. Biol.* 48, 609–639. doi: 10.1146/annurev.arplant.48.1.609

Duncan, O., Trosch, J., Fenske, R., Taylor, N. L., and Millar, A. H. (2017). Resource: mapping the *Triticum aestivum* proteome. *Plant J.* 89, 601–616. doi: 10.1111/tpj.13402

Dusenge, M. E., Duarte, A. G., and Way, D. A. (2019). Plant carbon metabolism and climate change: elevated CO_2 and temperature impacts on photosynthesis, photorespiration and respiration. *New Phytol.* 221, 32–49. doi: 10.1111/nph.15283

Ekele, J. U., Webster, R., Perez De Heredia, F., Lane, K. E., Fadel, A., and Symonds, R. C. (2025). Current impacts of elevated CO_2 on crop nutritional quality: a review using wheat as a case study. *Stress Biol.* 5, 34. doi: 10.1007/s44154-025-00217-w

Gámez, A. L., Vicente, R., Sanchez-Bragado, R., Jauregui, I., Morcuende, R., Goicoechea, N., et al. (2020). Differential flag leaf and ear photosynthetic performance under elevated (CO_2) conditions during grain filling period in durum wheat. *Front. Plant Sci.* 11, 587958. doi: 10.3389/fpls.2020.587958

Idso, S. B., and Idso, K. E. (2001). Effects of atmospheric CO_2 enrichment on plant constituents related to animal and human health. *Environ. Exp. Bot.* 45, 179–199. doi: 10.1016/s0098-8472(00)00091-5

IPCC (2023). "Summary for policymakers," in *Climate Change 2023: Synthesis Report. Contribution of Working Groups I, II and III to the Sixth Assessment Report of the Intergovernmental Panel on Climate Change*. Eds. H. Lee and J. Romero (IPCC, Geneva, Switzerland). doi: 10.59327/IPCC/AR6-9789291691647.001

Isaacson, T., Damasceno, C. M. B., Saravanan, R. S., Yonghua, H., Catalá, C., Saladié, M., et al. (2006). Sample extraction techniques for enhanced proteomic analysis of plant tissues. *Nat. Protoc.* 1, 769–774. doi: 10.1038/nprot.2006.102

Knopf, O., Castro, A., Bendig, J., Pude, R., Kleist, E., Poorter, H., et al. (2024). Field phenotyping of ten wheat cultivars under elevated CO_2 shows seasonal differences in chlorophyll fluorescence, plant height and vegetation indices. *Front. Plant Sci.* 14, 1304751. doi: 10.3389/fpls.2023.1304751

Kong, A. T., Leprevost, F. V., Avtonomov, D. M., Mellacheruvu, D., and Nesvizhskii, A. I. (2017). MSFragger: ultrafast and comprehensive peptide identification in mass spectrometry–based proteomics. *Nat. Methods* 14, 513–520. doi: 10.1038/nmeth.4256

Lan, X.-j., Tans, P., and Thoning, K. W. Trends in globally-averaged CO2 determined from NOAA global monitoring laboratory measurements. Available online at: https://gml.noaa.gov/ccgg/trends/gl_data.html (Accessed March 5, 2026).

Medina, S., Vicente, R., Amador, A., and Araus, J. L. (2016). Interactive effects of elevated [CO_2] and water stress on physiological traits and gene expression during vegetative growth in four durum wheat genotypes. *Front. Plant Sci.* 7, 1738. doi: 10.3389/fpls.2016.01738

Moore, B. D., Cheng, S. H., Sims, D., and Seemann, J. R. (1999). The biochemical and molecular basis for photosynthetic acclimation to elevated atmospheric CO_2. *Plant Cell Environ.* 22, 567–582. doi: 10.1046/j.1365-3040.1999.00432.x

Pandey, V., Sharma, M., Deeba, F., Maurya, V. K., Gupta, S. K., Singh, S. P., et al. (2017). Impact of elevated CO_2 on wheat growth and yield under free air CO_2 enrichment. *Am. J. Clim. Change* 6, 573–596. doi: 10.4236/ajcc.2017.64029

Patterson, F. L., and Ohm, H. W. (1975). Compensating ability of awns in soft red winter wheat. *Crop Sci.* 15, 403–407. doi: 10.2135/cropsci1975.0011183x001500030036x

Pavoković, D., Križnik, B., and Krsnik-Rasol, M. (2012). Evaluation of protein extraction methods for proteomic analysis of non-model recalcitrant plant tissues. *Croat. Chem. Acta* 85, 177–183. doi: 10.5562/cca1804

Perez-Riverol, Y., Bandla, C., Kundu, D. J., Kamatchinathan, S., Bai, J., Hewapathirana, S., et al. (2025). The PRIDE database at 20 years: 2025 update. *Nucl. Acids Res.* 53, D543–D553. doi: 10.1093/nar/gkae1011

Poorter, H., Knopf, O., Wright, I. J., Temme, A. A., Hogewoning, S. W., Graf, A., et al. (2022). A meta-analysis of responses of C_3 plants to atmospheric CO_2: dose–response curves for 85 traits ranging from the molecular to the whole-plant level. *New Phytol.* 233, 1560–1596. doi: 10.1111/nph.17802

Pratap, A., Taylor, N. L., Pal, M., Chinnusamy, V., and Siddique, K. H. M. (2025). Heat tolerance mechanisms in bread wheat: insights from flag leaves and spike tissues. *Plant Stress* 16, 100876. doi: 10.1016/j.stress.2025.100876

Racz, I., Hirişcău, D., Berindean, I., Kadar, R., Muntean, E., Tritean, N., et al. (2022). The influence of flag leaf removal and its characteristics on main yield components and yield quality indices on wheat. *Agron.* 12, 2545. doi: 10.3390/agronomy12102545

R Core Team (2025). *R: A Language and Environment for Statistical Computing* (Vienna, Austria: R Foundation for Statistical Computing). Available online at: https://www.R-project.org/ (Accessed May 1, 2026).

Song, K., Hong, S., and Shim, S. (2025). Responses of photosynthetic activity in flag leaves and spikes as well as seed development of wheat (*Triticum aestivum* L.) to artificial shading. *Agron.* 15, 2577. doi: 10.3390/agronomy15112577

Taub, D. R., and Wang, X. (2008). Why are nitrogen concentrations in plant tissues lower under elevated CO_2? A critical examination of the hypotheses. *J. Integr. Plant Biol.* 50, 1365–1374. doi: 10.1111/j.1744-7909.2008.00754.x

Teo, G. C., Polasky, D. A., Yu, F., and Nesvizhskii, A. I. (2021). Fast deisotoping algorithm and its implementation in the MSFragger search engine. *J. Proteome Res.* 20, 498–505. doi: 10.1021/acs.jproteome.0c00544

Tyanova, S., Temu, T., Sinitcyn, P., Carlson, A., Hein, M. Y., Geiger, T., et al. (2016). The Perseus computational platform for comprehensive analysis of (prote)omics data. *Nat. Methods* 13, 731–740. doi: 10.1038/nmeth.3901

Vicente, R., Bolger, A. M., Martínez-Carrasco, R., Pérez, P., Gutiérrez, E., Usadel, B., et al. (2019). De novo transcriptome analysis of durum wheat flag leaves provides new insights into the regulatory response to elevated CO_2 and high temperature. *Front. Plant Sci.* 10, 1605. doi: 10.3389/fpls.2019.01605

Wang, L., Feng, Z., and Schjoerring, J. K. (2013). Effects of elevated atmospheric CO_2 on physiology and yield of wheat (*Triticum aestivum* L.): a meta-analytic test of current hypotheses. *Agric. Ecosyst. Environ.* 178, 57–63. doi: 10.1016/j.agee.2013.06.013

Wang, W.-Q., Jensen, O. N., Møller, I. M., Hebelstrup, K. H., and Rogowska-Wrzesinska, A. (2018). Evaluation of sample preparation methods for mass spectrometry-based proteomic analysis of barley leaves. *Plant Methods* 14, 72. doi: 10.1186/s13007-018-0341-4

Wang, W., Tai, F., and Chen, S. (2008). Optimizing protein extraction from plant tissues for enhanced proteomics analysis. *J. Sep. Sci.* 31, 2032–2039. doi: 10.1002/jssc.200800087

Wang, N., Wu, X., Ku, L., Chen, Y., and Wang, W. (2016). Evaluation of three protein-extraction methods for proteome analysis of maize leaf midrib, a compound tissue rich in sclerenchyma cells. *Front. Plant Sci.* 7, 856. doi: 10.3389/fpls.2016.00856

Wiśniewski, J. R. (2016). Quantitative evaluation of filter aided sample preparation (FASP) and multienzyme digestion FASP protocols. *Anal. Chem.* 88, 5438–5443. doi: 10.1021/acs.analchem.6b00859

Wiśniewski, J. R. (2019). Filter aided sample preparation – a tutorial. *Anal. Chim. Acta* 1090, 23–30. doi: 10.1016/j.aca.2019.08.032

Wiśniewski, J. R., Zougman, A., Nagaraj, N., and Mann, M. (2009). Universal sample preparation method for proteome analysis. *Nat. Methods* 6, 359–362. doi: 10.1038/nmeth.1322

Wickham, H. (2016). *Ggplot2* (Cham, Switzerland: Springer International Publishing). doi: 10.1007/978-3-319-24277-4

Wu, X., Gong, F., and Wang, W. (2014). Protein extraction from plant tissues for 2DE and its application in proteomic analysis. *Proteomics* 14, 645–658. doi: 10.1002/pmic.201300239

Yu, F., Haynes, S. E., and Nesvizhskii, A. I. (2021). IonQuant enables accurate and sensitive label-free quantification with FDR-controlled match-between-runs. *Mol. Cell. Proteomics* 20, 100077. doi: 10.1016/j.mcpro.2021.100077

Zhu, C., Zhu, J., Zeng, Q., Liu, G., Xie, Z., Tang, H., et al. (2009). Elevated CO_2 accelerates flag leaf senescence in wheat due to ear photosynthesis which causes greater ear nitrogen sink capacity and ear carbon sink limitation. *Funct. Plant Biol.* 36, 291–299. doi: 10.1071/fp08269